Chapter 8

Control of Fluorescence and Photosensitized Singlet Oxygen-Generating Activities of Porphyrins by DNA: Fundamentals for "Theranostics"

Kazutaka Hirakawa

Additional information is available at the end of the chapter

http://dx.doi.org/10.5772/67882

Abstract

The purpose of this chapter is the brief review of the fundamental study of porphyrin "theranostics" by DNA. Porphyrins have been studied as photosensitizer for photodynamic cancer therapy. The activity control of fluorescence emission and photosensitized singlet oxygen generation by porphyrins using the interaction with DNA is the initial step in achieving theranostics. To control these photochemical activities, several types of electron donor–connecting porphyrins were designed and synthesized. The theoretical calculations speculated that the photoexcited state of these porphyrins can be deactivated via intramolecular electron transfer, forming a charge–transfer state. The electrostatic interaction between the cationic porphyrin and DNA predicts a rise in the energy of the charge–transfer state, leading to the inhibition of electron transfer quenching. Pyrene– and anthracene–connecting porphyrins showed almost no fluorescence in an aqueous solution. Furthermore, these porphyrins could not photosensitize singlet oxygen generation. These porphyrins bind to a DNA groove through an electrostatic interaction, resulting in the increase of fluorescence intensity. The photosensitized singlet oxygen–generation activity of DNA–binding porphyrins could also be confirmed. On the other hand, several other porphyrins could not demonstrate the activity control properties. To realize effective activity control, a driving force of more than 0.3 eV is required for the porphyrins.

Keywords: cationic porphyrin, DNA, singlet oxygen, electron transfer, fluorescence

1. Introduction

"Theranostics" [1–3] is a relatively new technical term that includes the meanings of therapeutics and diagnostics [4–9]. The purpose of this review is an introduction of examples of theranostics using porphyrins. Porphyrins can emit relatively strong fluorescence in the wavelength range of visible light and generate singlet oxygen ($^1O_2$), an important reactive oxygen species [10]. Singlet oxygen is generated through energy transfer from the triplet excited (T_1) state of the photosensitizer to the ground state of oxygen molecules ($^3O_2$) [11–13]. Fluorescence imaging is the fundamental mechanism of photodynamic diagnosis (PDD) [14], and $^1O_2$ is the important reactive species for photodynamic therapy (PDT) [15]. PDT is a less-invasive and promising treatment for cancer and other nonmalignant conditions [4–9, 15]. In general, a mechanism of PDT is the oxidation of biomacromolecules, including DNA and proteins, by $^1O_2$, which is generated through energy transfer from the excited photosensitizer to oxygen molecules. Porphyrins have been extensively studied as photosensitizers of PDT. Porfimer sodium [16] and talaporfin sodium [17] are especially important clinical drugs used in PDT (**Figure 1**). The control of the photoexcited state of porphyrins by targeting molecules or surrounding environments is the fundamental mechanism of theranostics. In this chapter, the fundamental studies about DNA-targeting porphyrin theranostics are introduced. DNA is a potentially important target molecule of PDT. Indeed, many DNA-targeting drugs have been studied and reported [18–20].

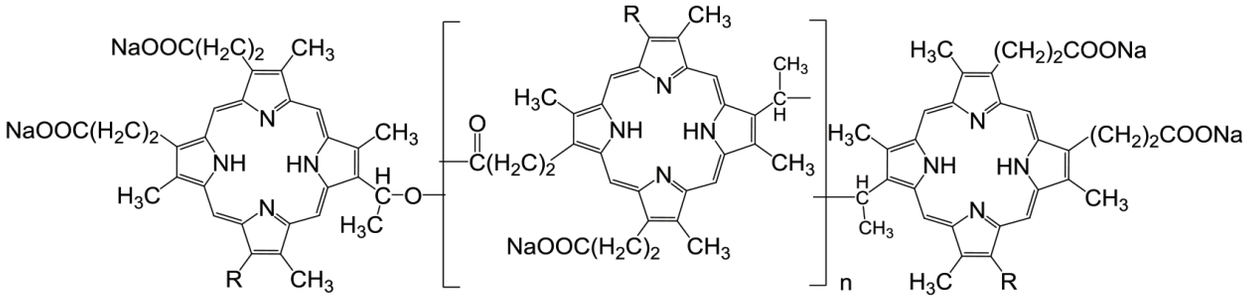

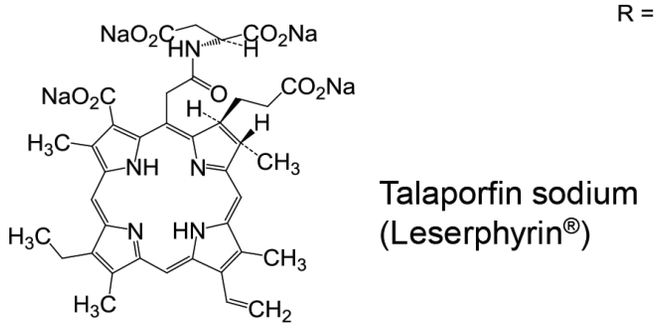

Figure 1. Structures of examples of PDT photosensitizers, porfimer sodium and talaporfin sodium.

1.1. Photodynamic therapy

Photodynamic therapy is a promising and less-invasive treatment for cancer [4-9, 15]. Porphyrins are used as photosensitizers of PDT (**Figure 2**). The abovementioned porphyrins, porfimer sodium [16] and talaporfin sodium [17], are especially important photosensitizers. Under visible light irradiation, especially long wavelength visible light (wavelength > 650 nm), an administered porphyrin photosensitizer generates $^1O_2$ through energy transfer to an oxygen molecule (the type II mechanism) [21]. Since human tissue has a relatively high transparency for visible light, especially red light, visible light rarely demonstrates side effects. Critical targets of $^1O_2$ include mitochondria and enzyme proteins; DNA is also an important target for PDT [22–26]. In general, the $^1\sum_g^+$ state of $^1O_2$ ($^1O_2(^1\sum_g^+)$) is mainly formed through the energy transfer from the T_1 state of photosensitizers. This state of $^1O_2$ has relatively high energy, about 1.6 eV, corresponding to the ground state; however, the lifetime is very short (several picoseconds). The $^1O_2(^1\sum_g^+)$ is rapidly converted to the $^1\Delta_g$ state ($^1O_2(^1\Delta_g)$), which has a relatively long lifetime (several microseconds). Therefore, $^1O_2(^1\Delta_g)$ is a more important reactive oxygen species of PDT. In this chapter, $^1O_2$ indicates $^1O_2(^1\Delta_g)$ without explanation. This biomacromolecule damage induces apoptosis and/or necrosis. Apoptosis, a programed death of cancer cells, is considered the main mechanism of PDT [15, 27]. Necrosis also contributes to the mechanism of cell death in the case of severe damage of biomacromolecules by a high dose of photosensitizers and intense photoirradiation [15]. In the case of DNA-targeting PDT, $^1O_2$ selectively oxidizes guanines. The main oxidized product of guanine is 8-oxo-7,8-dihydrodeoxyguanine [28–30].

1.2. Aminolevulinic acid

One of the most important practical applications of theranostics is the method using the administration of 5-aminolevulinic acid (5-ALA, see **Figure 3**) [31–33]. Although the strategy of 5-ALA theranostics is different from the activity control of the photosensitizer by target molecules mentioned in this chapter, this method is important for cancer theranostics. 5-ALA is the source of protoporphyin IX (PPIX) in human cells. In the normal cell, PPIX is converted into iron porphyrin, which cannot emit fluorescence. However, in cancer cells,

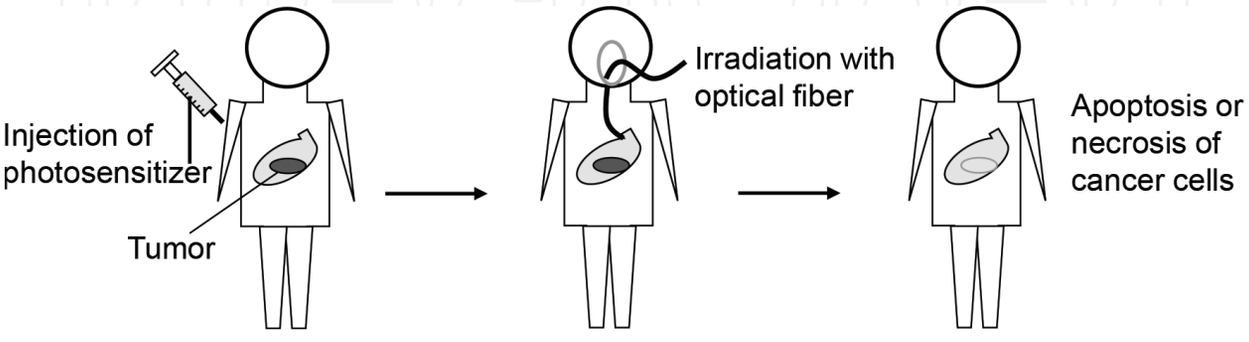

Figure 2. A general procedure of PDT.

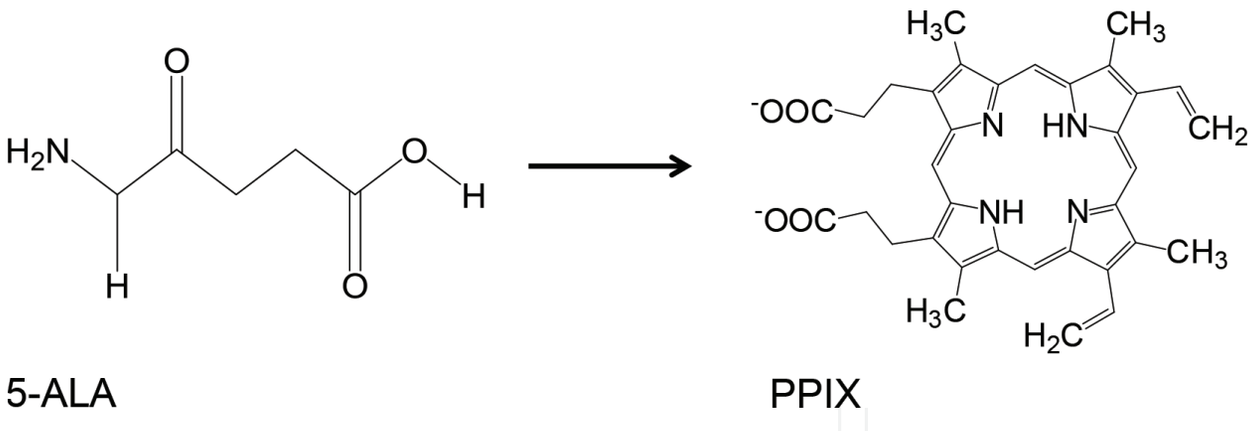

Figure 3. PPIX formation from 5-ALA.

PPIX is selectively concentrated. Several mechanisms for this cancer-selective concentration of PPIX have been speculated [34, 35]. Because PPIX demonstrates relatively strong red fluorescence around 650 nm and under blue light irradiation around 450 nm, this phenomenon can be applied to cancer diagnosis. Indeed, the diagnosis of 5-ALA is clinically applied to the treatment of cancer, for example, malignant brain tumors [36, 37] and bladder cancer [38]. Furthermore, PPIX can photosensitize $^1O_2$ generation. Although the efficiency of $^1O_2$ generation by free PPIX is relatively low, the $^1O_2$-generating activity of PPIX can be increased depending on the environment [39]. These properties of 5-ALA and PPIX can be used in cancer theranostics.

1.3. Strategy of porphyrin theranostics with target biomolecules

Figure 4 shows the energy diagram of the relaxation process of photoexcited porphyrins and theranostics. The singlet excited (S_1) state of the photosensitizer (Sens*(S_1)) is formed by photoirradiation. In the OFF state, without the target biomacromolecules, the S_1 state is rapidly quenched, and the excitation energy is dispersed as heat. For example, intramolecular

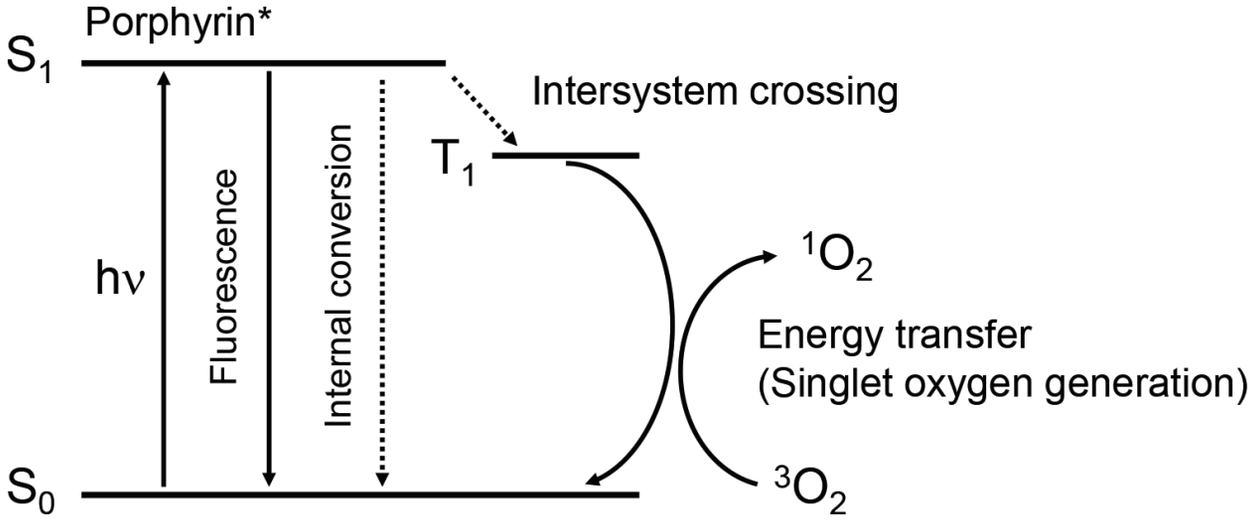

Figure 4. An energy diagram of the relaxation process of photoexcited porphyrin.

http://dx.doi.org/10.5772/67882

electron transfer is a convenient pathway for the quenching to control photochemical activity. In the presence of target molecules, the interaction between the photosensitizer (Sens) and the target molecule inhibits the intramolecular electron transfer. The S_1 state with target molecules can emit fluorescence (ON state). In the case of porphyrin, the quantum yield of fluorescence (Φ_f) is almost 10% for a relatively intense case. In addition, the intersystem crossing proceeds with a relatively large quantum yield (Φ_T); more than 50% is a sufficient value for the Φ_T. These processes are expressed by the following equations:

$$\text{Sens} + h\nu \rightarrow \text{Sens}^*(S_1) \quad (1)$$

$$\text{Sens}^*(S_1) \rightarrow \text{Sens} + \text{heat}\ (\text{Activity: OFF}) \quad (2)$$

$$\text{Sens}^*(S_1) \rightarrow \text{Sens} + h\nu\ (\text{Activity: ON}) \quad (3)$$

$$\text{Sens}^*(S_1) \rightarrow \text{Sens}^*(T_1)\ (\text{Activity: ON}) \quad (4)$$

$$\text{Sens}^*(T_1) + {}^3O_2 \rightarrow {}^1O_2\ (\text{Activity: ON}) \quad (5)$$

where Sens*(T_1) is the T_1 state of the photosensitizer. **Figure 5** shows the scheme of the activity control of photosensitizer by DNA. In the case of DNA, several forms of the binding interaction can be speculated [40–43]. For example, an electrostatic interaction can switch the activity of photosensitizers.

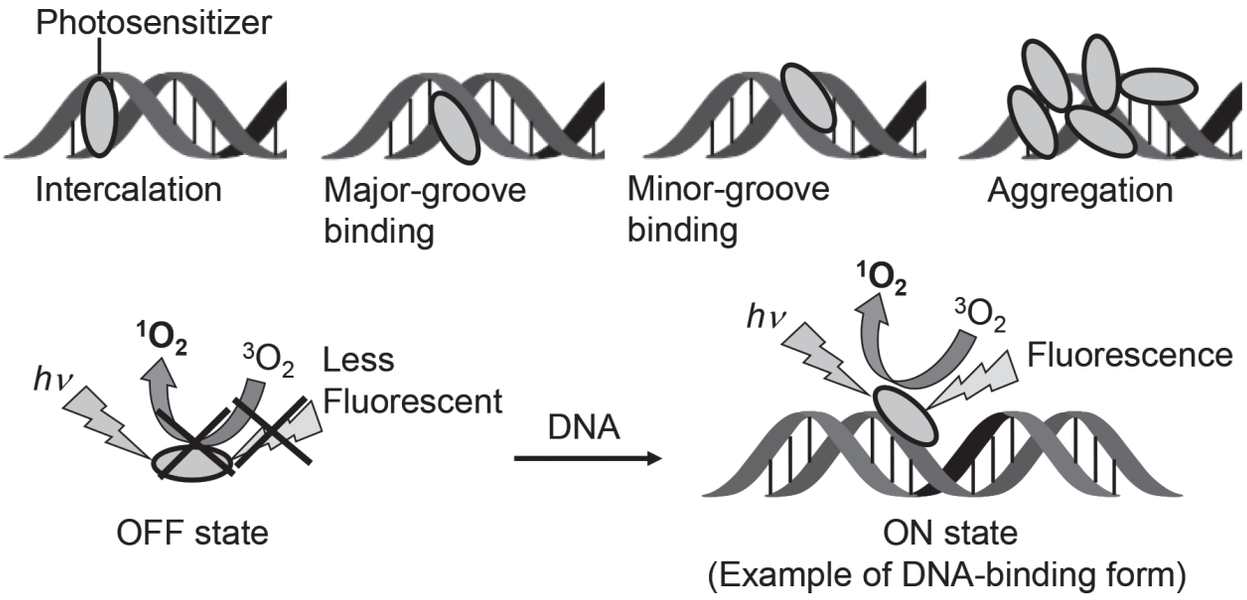

Figure 5. Scheme of the binding interaction between photosensitizers and DNA and the activity switching of photosensitizers through the interaction with DNA.

2. Control of fluorescence and $^1O_2$-generating activity of alkaloids by DNA

Photosensitized DNA damage is an important process in medical applications of photochemical reactions [44, 45]. In this section, the activity control of naturally occurring photosensitizers

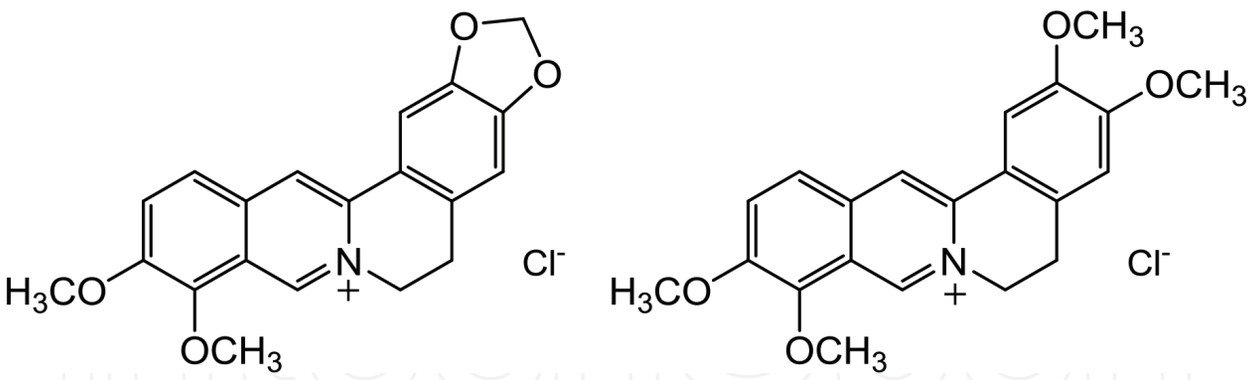

Figure 6. Structures of berberine (left) and palmatine (right).

is introduced. Berberine and palmatine are alkaloids (**Figure 6**). These molecules barely emit fluorescence. The S_1 state of these alkaloids deactivates within 40~50 ps through intramolecular electron transfer in aqueous solution [46–48]. Since these alkaloids are cationic compounds, in the presence of DNA, an anionic polymer, berberine and palmatine spontaneously bind to the DNA strand through electrostatic interaction. Indeed, it was reported that berberine preferentially binds to adenine-thymine–rich minor grooves [49]. The minor groove bindings of berberine and palmatine could be speculated from molecular mechanics calculation [48]. The interaction between these alkaloids and DNA was investigated using oligonucleotides of the adenine-thymine sequence (AATT: $d(AAAATTTTAAAATTTT)_2$) and the guanine-containing sequence (AGTC: $d(AAGCTTTGCAAAGCTT)_2$) [48]. The apparent binding constant can be easily estimated from the absorption spectral change of these alkaloids, and the reported values are relatively high [48]. The fluorescence intensity of berberine and palmatine was markedly increased in the presence of DNA. The Φ_f and the fluorescence lifetimes (τ_f) of berberine and palmatine were markedly increased through interaction with DNA (**Table 1**).

Furthermore, the $^1O_2$-generation activity of berberine and palmatine was markedly enhanced by DNA. In aqueous solution, berberine and palmatine hardly photosensitize $^1O_2$ generation.

Alkaloid	DNA	Φ_f	τ_f/ns (ratio)			Φ_Δ
Berberine	Without	<0.001	0.05			nd
	AATT	0.093	0.30 (0.30)	3.7 (0.42)	11.9 (0.28)	0.066
	AGTC	0.043	0.12 (0.60)	1.6 (0.32)	8.0 (0.08)	0.036
Palmatine	Without	<0.001	0.04			nd
	AATT	0.054	0.16 (0.39)	2.3 (0.45)	6.9 (0.16)	0.044
	AGTC	0.031	0.14 (0.54)	1.4 (0.37)	5.9 (0.09)	0.030

The fluorescence properties were examined in a 10-mM sodium phosphate buffer (pH = 7.6). The Φ_Δ values were determined in deuterium oxide. These values were reported in the literature [48].

Table 1. Fluorescence and photosensitized $^1O_2$-generating activities of berberine and palmatine in the absence or presence of DNA.

However, in the presence of DNA, the near-infrared emission at around 1270 nm, assigned to the radiative deactivation of $^1O_2$ into its ground state, was clearly observed under photoirradiation of these alkaloids. The estimated quantum yield of $^1O_2$ generation (Φ_Δ) using the reference compound, methylene blue (Φ_Δ = 0.52) [50], depended on the sequence and decreased for the guanine-containing sequence (**Table 1**). These characteristics are the fundamental mechanisms of theranostics. The theranostics mechanism of berberine and palmatine can be explained as follows:

1. The photoexcited states of these compounds are rapidly quenched through intramolecular electron transfer. These alkaloids consist of the *iso*-quinoline moiety and dialkoxybenzene moiety (**Figure 7**). The *iso*-quinoline moiety can fluoresce and photosensitize $^1O_2$ generation, and the dialkoxybenzene moiety can act as an electron-donating site.
2. The electrostatic interaction with DNA increases the Gibbs free energy (ΔG) of the intramolecular electron transfer. In addition, the hydrophobic environment of the DNA strand [51, 52] is unfavorable for the intramolecular electron transfer. Consequently, the lifetime of the S_1 state becomes markedly long compared with that without DNA.
3. Fluorescence intensity and the intersystem crossing yield are increased, resulting in the enhancement of energy transfer to the oxygen molecule to generate $^1O_2$.

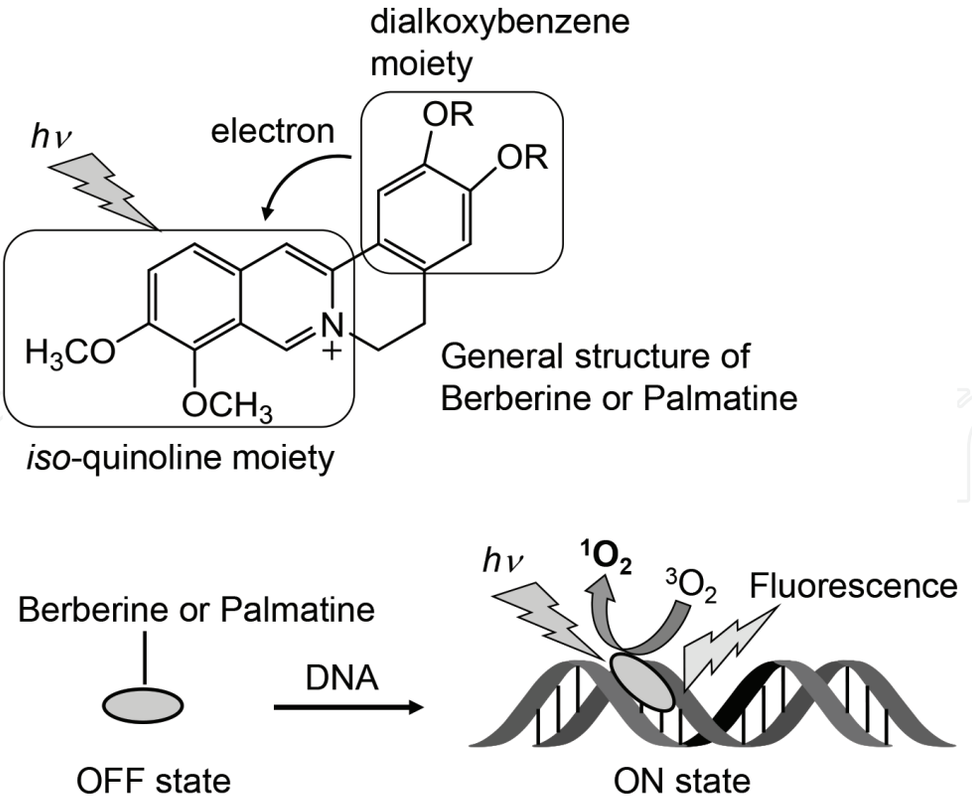

Figure 7. Intramolecular electron transfer in the S_1 state of berberine and palmatine and the activity switching by DNA.

3. DNA-targeting porphyrin theranostics

The abovementioned mechanisms of berberine and palmatine can be applied to porphyrin theranostics. For this purpose, cationic porphyrins are useful because they can be incorporated into the cell nucleus and can photosensitize cellular DNA damage [53]. Furthermore, cationic porphyrins can bind to a DNA strand through electrostatic interaction, similar to berberine and palmatine. For example, anionic water-soluble porphyrin PPIX hardly induces cellular and isolated DNA damage, whereas tetrakis(*N*-methyl-4-pyridinio) porphyrin (TMPyP, see **Figure 8**) effectively photosensitizes the guanine-specific oxidation of cellular and isolated DNA through $^1O_2$ generation. Thus, electron donor-connecting cationic porphyrins were designed and synthesized to realize porphyrin theranostics.

3.1. Binding interaction with DNA and cellular and isolated DNA-damaging activity of water-soluble porphyrins

The effect of a DNA microenvironment on the photosensitized reaction of water-soluble porphyrin derivatives, TMPyP and its zinc complex (ZnTMPyP, see **Figure 8**), was reported [42]. The main driving force of DNA binding is electrostatic interaction. The binding form between these porphyrins and DNA depends on the concentration ratio of porphyrins and DNA bases. In the presence of a sufficient concentration of DNA, TMPyP mainly intercalates to the DNA strand, whereas ZnTMPyP binds to the DNA groove. An electrostatic interaction with DNA raises the redox potential of the binding porphyrins, resulting in suppression of the photoinduced electron transfer from an electron donor to the DNA-binding porphyrins, whereas the electron transfer from the porphyrins to the electron acceptor was enhanced.

Cellular DNA damage by photoirradiated water-soluble porphyrins, TMPyP and PPIX was examined [53]. TMPyP and PPIX induced apoptosis in the human leukemia HL-60 cell

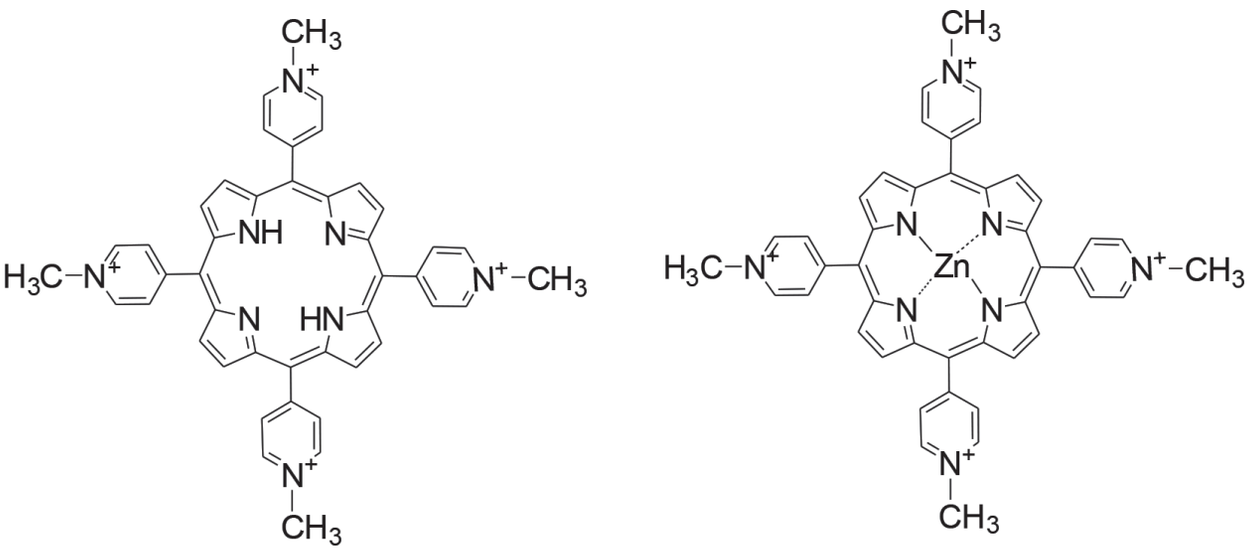

Figure 8. Structures of TMPyP (left) and ZnTMPyP (right).

under photoirradiation [53]. TMPyP is incorporated in the cell nucleus and photosensitizes cellular DNA oxidation, whereas PPIX hardly demonstrates cellular DNA-damaging ability. In the case of an isolated DNA fragment, photoexcited TMPyP effectively oxidized most guanine residues, whereas little or no DNA damage was observed in the PPIX case [53]. Consequently, a TMPyP cationic porphyrin should be useful as a DNA-targeting photosensitizer.

3.2. Design and synthesis of electron donor-connecting porphyrin

Molecular orbital (MO) calculation suggests that pyrene-connecting TMPyP (PyTPP, see **Figure 9**) can be used for porphyrin theranostics in a DNA microenvironment [54]. **Figure 9** shows the optimized structures of PyTPP and AnTPP and their highest-occupied MOs (HOMO). The binding action of PyTPP into the DNA major groove was suggested, and the apparent association constants, estimated from the relationship between the absorbance change and the DNA concentration, are relatively large (1.0×10^6 M^{-1} and 8.3×10^5 M^{-1} for AATT and AGTC, respectively). The fluorescence spectrum and its lifetime measurements showed that this porphyrin demonstrates almost no fluorescence in

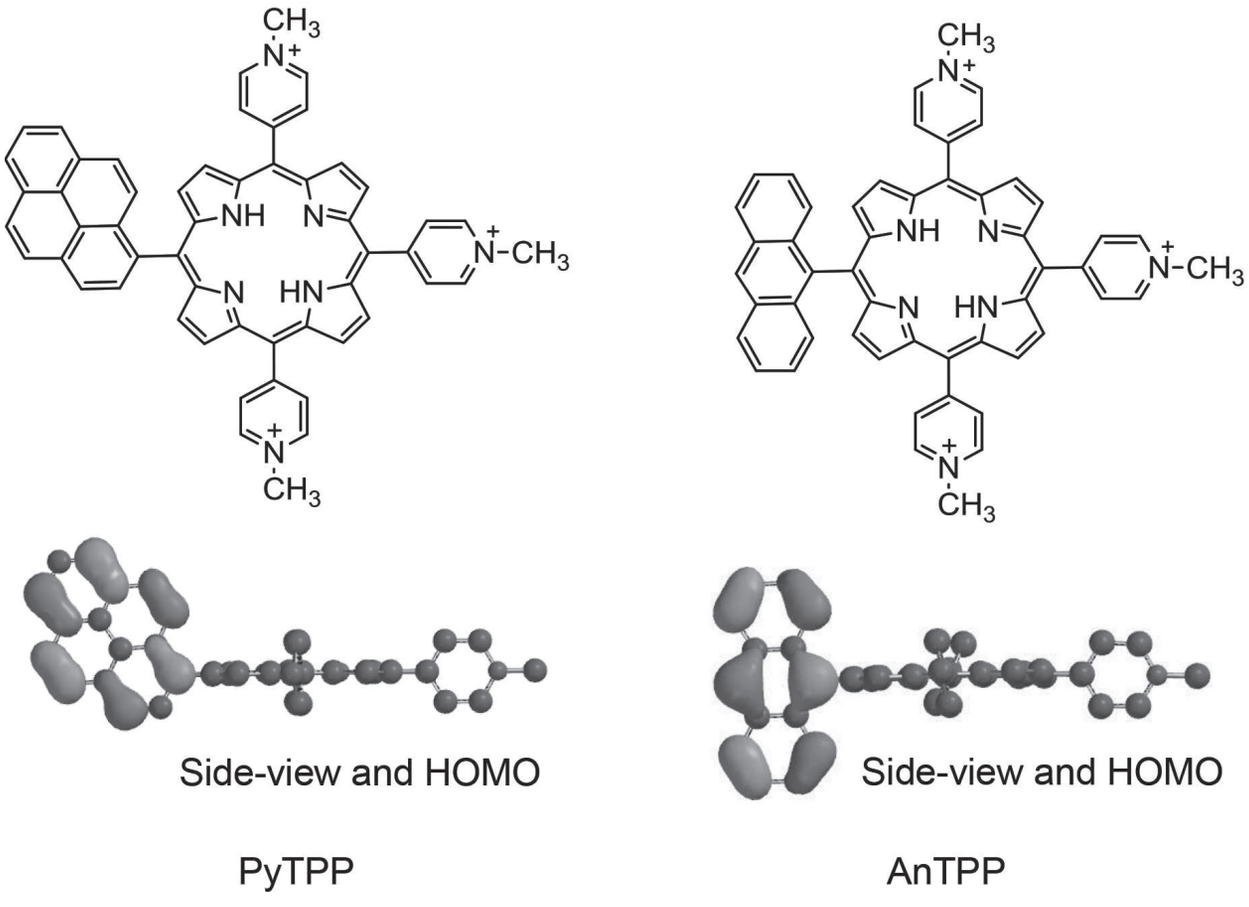

Figure 9. Structures of PyTPP (left) and AnTPP (right). The side-view structures and the HOMO of these porphyrins were obtained by the MO calculation at the Hartree-Fock 6-31G* level.

aqueous solution (Φ_f < 0.001, see **Table 2**) because of the rapid intramolecular electron transfer. The electron-accepting ability of the porphyrin moiety is decreased by the electrostatic interaction with DNA. In the presence of DNA, the fluorescence intensity was markedly increased (Φ_f is 0.12 and 0.10 in the presence of 50-μM base pairs AATT and AGTC, respectively). In addition, the typical near-infrared emission spectrum of $^1O_2$ was clearly observed during the photoexcitation of PyTPP with DNA, whereas the emission was not observed without DNA. The estimated Φ_Δ by PyTPP-DNA was 0.051 and 0.038 in the presence of 50-μM base pairs AATT and AGTC, respectively. In conclusion, the S_1 state of PyTPP is effectively quenched by the pyrenyl moiety. The interaction with DNA suppresses this electron transfer, leading to the enhancement of fluorescence emission. The intersystem crossing is also enhanced and makes $^1O_2$ generation possible.

Porphyrin	DNA	Φ_f	τ_f/ns (ratio)		Φ_Δ
PyTPP [54]	Without	<0.001	0.04		nd
	AATT	0.12	12.0		0.051
	AGTC	0.10	10.6 (0.62)	2.8 (0.38)	0.038
AnTPP [55]	Without	<0.001	0.04		nd
	AATT	0.098	10.4 (0.88)	3.6 (0.12)	0.22
	AGTC	0.077	10.6 (0.79)	2.8 (0.21)	0.17

The fluorescence properties and the Φ_Δ values were examined in a 10-mM sodium phosphate buffer (pH = 7.6). These values were reported in the literature [54, 55].

Table 2. Fluorescence and photosensitized $^1O_2$-generating activities of PyTPP and AnTPP in the absence or presence of DNA.

3.3. Improvement of the activity control using anthracene

In the abovementioned case of PyTPP, Φ_f can be recovered to a value comparable to that of TMPyP. However, Φ_Δ is significantly smaller than that of TMPyP. A relatively small Φ_Δ value might be due to the self-oxidation of PyTPP through the photosensitized $^1O_2$ generation. Since an electron donor is easily oxidized by $^1O_2$, the connection of the electron donor tends to decrease the apparent yield of $^1O_2$ generation. $^1O_2$ may oxidize the pyrene moiety through the Diels-Alder reaction. To avoid this self-oxidation, anthracene-connecting TMPyP (AnTPP, see **Figure 9**) was designed and synthesized [55]. The optimized structure of AnTPP according to MO calculation suggested that oxidation of the anthracene moiety directly connecting at the mesoposition of the porphyrin is difficult because of steric hindrance, resulting in recovery of the $^1O_2$ yield. In addition, the MO calculation indicated the steric rotational hindrance of the anthracene moiety around the mesoposition of the porphyrin, which keeps the two π-electronic systems nearly orthogonal to each other. This calculation also showed that the activity control of fluorescence and $^1O_2$ generation of this porphyrin through an interaction with DNA is possible.

In aqueous solution, AnTPP barely demonstrates fluorescence emission (Φ_f < 0.001) and $^1O_2$ generation (**Table 2**). The observed fluorescence lifetime (<40 ps) indicates the rapid intramolecular electron transfer in the S_1 state of the porphyrin moiety of AnTPP. AnTPP also binds to the DNA strand, mainly the minor groove, and the reported association constant is relatively large (~10^6 M^{-1}). DNA-binding AnTPP demonstrates a relatively strong fluorescence and long fluorescence lifetime comparable to those of the reference porphyrin without an electron donor. Furthermore, the $^1O_2$-generating activity of AnTPP is recovered by DNA. The estimated values of Φ_Δ relative to that of methylene blue are 0.22 and 0.17 for the AATT- and AGTC-binding forms of AnTPP, respectively (**Table 2**). The observed values of Φ_Δ are significantly larger than those of PyTPP. These results suggest that the $^1O_2$-generating activity of AnTPP has improved due to the inhibition of self-oxidation by the generated $^1O_2$.

3.4. Phenanthrene-connecting cationic porphyrin

Phenanthrene was also used as the electron donor of the cationic porphyrin [56]. However, the activity control of the phenanthrene-connecting porphyrin (PhenTPP, see **Figure 10**) was not successful. The MO calculation showed the HOMO location on the phenanthryl moiety of PhenTPP and predicted the similarity of this porphyrin property to the abovementioned PyTPP and AnTPP. However, the observed values of Φ_f and τ_f without DNA are 0.028 and 5.8 ns (89%) and 2.7 ns (11%), respectively, indicating insufficient quenching of the S_1 state by phenanthrene. Furthermore, the estimated value of Φ_Δ by PhenTPP without DNA is large (0.38). Consequently, the activity control of this type of porphyrin by phenanthrene is not appropriate. This result can be explained by the relatively small driving force of the intramolecular electron transfer ($-\Delta G$ = 0.18 eV). The driving force dependence of this electron transfer is discussed in the next section in detail.

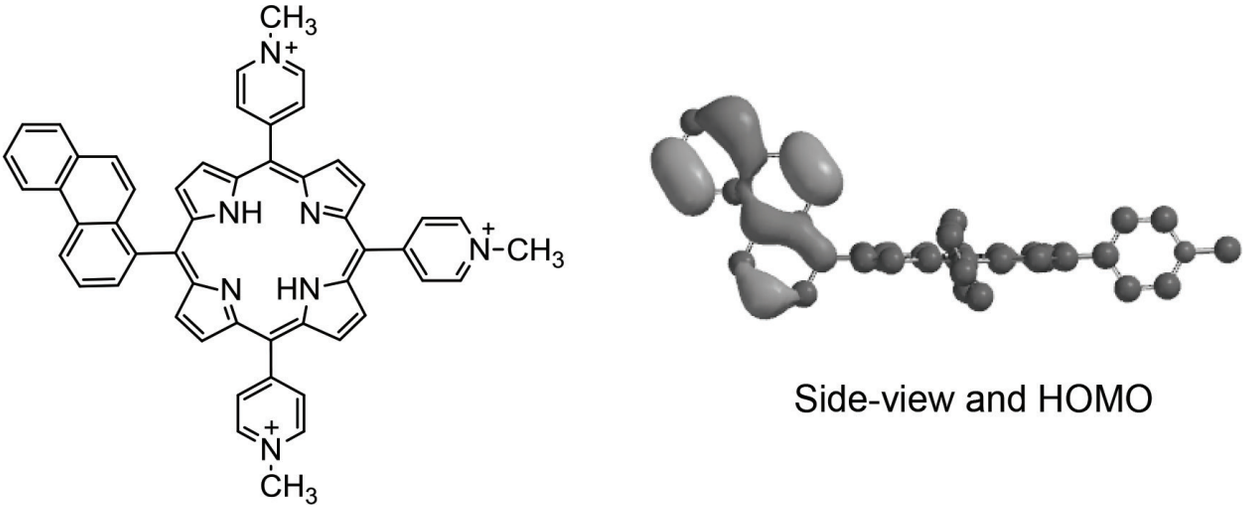

Figure 10. A structure of PhenTPP. The side-view structure and the HOMO of PhenTPP (right) were obtained by the MO calculation at the Hartree-Fock 6-31G* level.

4. Factors governing the activity control of the photochemical property of the electron donor-connecting porphyrin

As mentioned above, the controls of fluorescence intensity and $^1O_2$-generating activities of the cationic porphyrin connecting to the pyrenyl and anthryl groups by DNA could be successfully established. On the other hand, in the case of phenanthrylporphyrin, the S_1 state of this porphyrin could not be deactivated through intramolecular electron transfer because the electron-donating property of the phenanthryl moiety was insufficient [56]. To investigate the factors governing the activity control of the electron donor-connecting porphyrins, two types of electron donor-connecting porphyrins, *meso*-(1-naphthyl)-tris(*N*-methyl-*p*-pyridinio)porphyrin (1-NapTPP) and *meso*-(2-naphthyl)-tris(*N*-methyl-*p*-pyridinio)porphyrin (2-NapTPP) (**Figure 11**), were designed and synthesized [57].

These naphthylporphyrins, 1-NapTPP and 2-NapTPP, spontaneously bind to double-stranded DNA [57]. The electrostatic force between cationic porphyrins and the anionic DNA strand, as well as the hydrophobic interaction, can be speculated as the driving force of the binding interaction. In the presence of relatively small concentrations of DNA, these naphthylporphyrins aggregate around the DNA strand because their water solubility is relatively low. In the presence of a sufficient concentration of DNA, these naphthylporphyrins can form

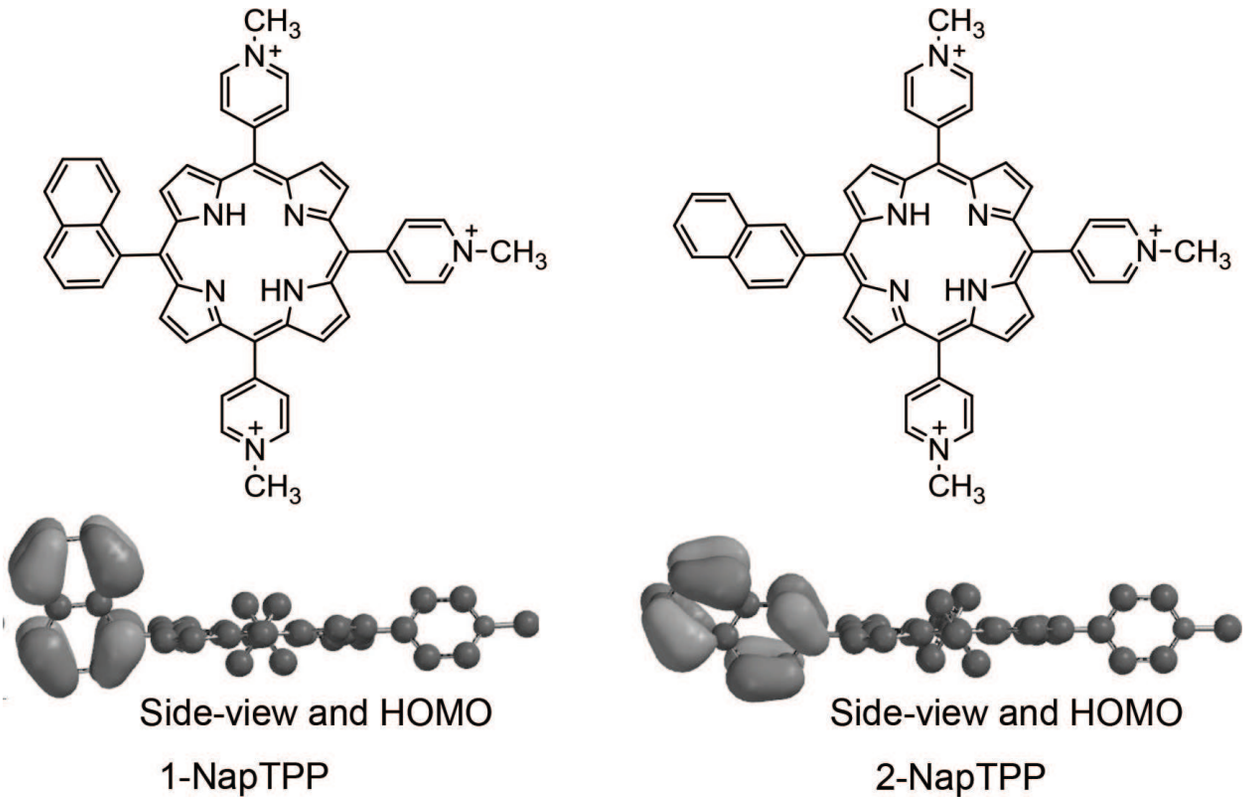

Figure 11. Structures of 1-NapTPP (left) and 2-NapTPP (right). The side-view structures and the HOMO of these porphyrins were obtained by the DFT calculation at the B3LYP/6-31G* level.

a stable complex with the DNA strand. The estimated binding constants were relatively large (more than 10^6 M^{-1}). The binding constants for those of the adenine-thymine sequence only were larger than those of the guanine-cytosine-containing sequences.

Similar to the other electron donor-connecting cationic porphyrin cases, the calculations by the density functional treatment (DFT) demonstrated that the photoexcited states of these naphthylporphyrins are deactivated through intramolecular electron transfer from their naphthalene moieties to the S_1 states of the porphyrin moieties [57]. However, the S_1 state of these porphyrins was hardly quenched by their naphthalene moieties. The Φ_Δ values of these naphthylporphyrins are also relatively large without DNA (**Table 3**). The orthogonal position of these naphthalene moieties and the porphyrin rings and the relatively small values of $-\Delta G$ of the intramolecular electron transfer (0.11 and 0.07 eV for 1- and 2-NapTPP, respectively) are not appropriate for electron-transfer quenching. The relationship between the estimated intramolecular electron transfer rate constants (k_{ET}), which are reported in the literature [57], and the driving force ($-\Delta G$ values) is plotted using the reported values and shown in **Figure 12**. The plots were analyzed by Marcus theory [58, 59] using the following equation:

$$k_{ET} = \sqrt{\frac{4\pi^3}{h^2 \lambda K_B T}} V^2 \exp \frac{-(\Delta G^* + \lambda)^2}{4\lambda K_B T} \quad (6)$$

where h is Planck's constant, λ is the reorganization energy, K_B is the Boltzmann constant, V is the electronic coupling matrix element, and T is the absolute temperature. Observed several components of the τ_f for 1- and 2-NapTPP suggest the different conformations. Therefore, the different V values were considered to explain slow electron transfer and relatively fast electron transfer. The analyzed values of V were significantly smaller than those of other directly connecting electron donor-acceptor molecular systems [60–62], suggesting that the interaction between the electron donor and the porphyrin ring is small, possibly due to the orthogonal structure. This plot suggests that a $-\Delta G$ of more than 0.3 eV is required for effective quenching through electron transfer in these types of porphyrin systems.

Porphyrin	DNA	Φ_f	τ_f/ns (ratio)			Φ_Δ
1-NapTPP	Without	0.030	6.1 (0.76)	3.7 (0.22)	0.2 (0.02)	0.26
	AATT	0.062	12.3 (0.95)	2.2 (0.03)	0.1 (0.02)	0.20
	AGTC	0.048	11.3 (0.89)	4.1 (0.09)	0.1 (0.02)	0.19
2-NapTPP	Without	0.030	3.5 (0.94)	1.3 (0.06)		0.43
	AATT	0.092	11.7 (0.89)	5.8 (0.10)	0.9 (0.01)	0.46
	AGTC	0.072	10.5 (0.76)	4.9 (0.23)	0.8 (0.01)	0.37

The fluorescence properties and the Φ_Δ values were examined in a 10-mM sodium phosphate buffer (pH 7.6). These values were reported in the literature [57].

Table 3. Fluorescence and photosensitized $^1O_2$-generating activities of 1-NapTPP and 2-NapTPP in the absence or presence of DNA.

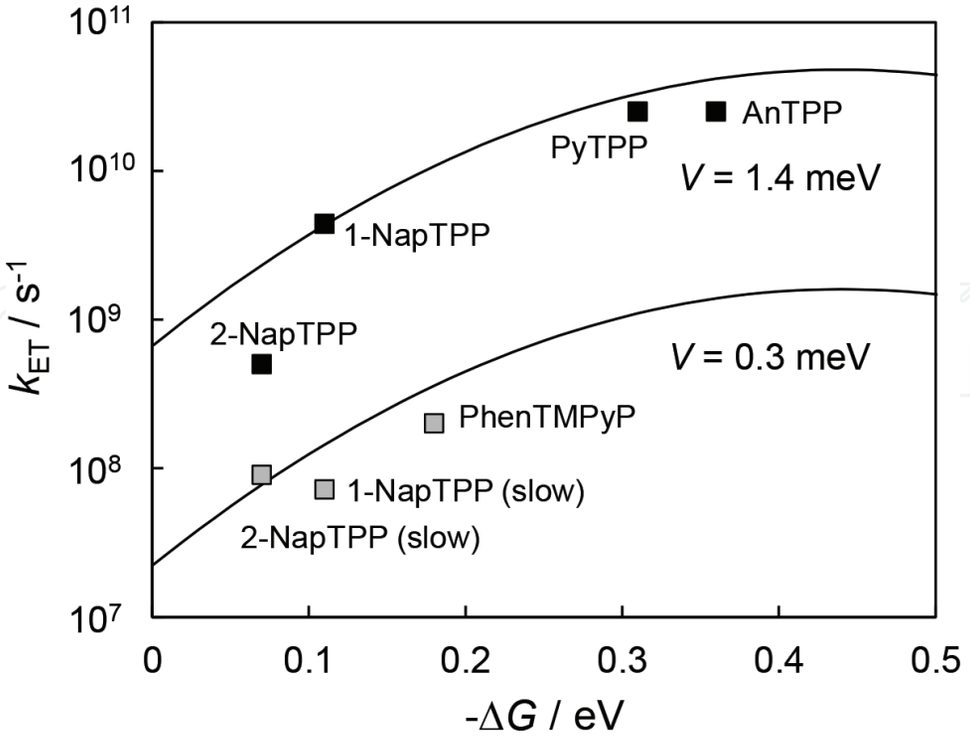

Figure 12. Relationship between the electron transfer rate and the driving force. The plots of 1-NapTPP (slow) and 2-NapTPP (slow) were calculated by using the components of their long fluorescence lifetime. These curves were calculated by the Marcus equation using two appropriate values of *V*. This relationship is reported in the literature [57].

5. Conclusions

Naturally occurring photosensitizers, berberine and palmatine, demonstrate important photochemical properties. In aqueous solution, the S_1 state of these compounds was rapidly quenched through an intramolecular electron transfer. These compounds bind to a DNA strand through electrostatic interaction, resulting in inhibition of electron transfer-mediated quenching. This interaction makes the fluorescence emission and $^1O_2$ generation by these compounds possible. A similar mechanism can be applied to the cationic porphyrin. TMPyP cationic porphyrins can be incorporated into the cell nucleus and can photosensitize guanine-specific oxidation by $^1O_2$ generation, leading to apoptosis. Therefore, the electron donor-connecting TMPyP porphyrins can be considered as model photosensitizers for theranostics. For example, PyTPP and AnTPP were designed and synthesized. The activity control of fluorescence and $^1O_2$ generation by these cationic porphyrins could be successfully established. However, the activity control of phenanthrene- and naphthalene-connecting porphyrins is insufficient because of their slow intramolecular electron transfer rate. These results suggest that a driving force of more than 0.3 eV is required for sufficiently fast electron transfer in similar porphyrin types. These studies demonstrate the possibility of porphyrin theranostics through control of the S_1 state of the porphyrin ring by the electron-donating moiety and interaction with DNA, one of the most important target biomacromolecules for cancer therapy.

Acknowledgements

The author wishes to thank Professor Shigetoshi Okazaki and Professor Toru Hirano (Hamamatsu University School of Medicine), Professor Yoshinobu Nishimura and Professor Tatsuo Arai (University of Tsukuba), Emeritus Professor Yoshio Nosaka (Nagaoka University of Technology), Mr. Takashi Yamada, Ms. Mari Harada, Mr. Yusuke Ito, and Mr. Makoto Taguchi (Shizuoka University) for their collaborations. These works were partially supported by JSPS KAKENHI from the Ministry of Education, Culture, Sports, Science and Technology of the Japanese Government.

Author details

Kazutaka Hirakawa

Address all correspondence to: hirakawa.kazutaka@shizuoka.ac.jp

Department of Engineering, Graduate School of Integrated Science and Technology, Shizuoka University, Hamamatsu, Shizuoka, Japan

Department of Optoelectronics and Nanostructure Science, Graduate School of Science and Technology, Shizuoka University, Hamamatsu, Shizuoka, Japan

References

[1] Rai P, Mallidi S, Zheng X, Rahmanzadeh R, Mir Y, Elrington S, Khurshid A, Hasan T. Development and applications of photo-triggered theranostic agents. Advanced Drug Delivery Reviews. 2010;**62**:1094–1124. doi:10.1016/j.addr.2010.09.002

[2] Ai X, Mu J, Xing B. Recent advances of light-mediated theranostics. Theranostics. 2016;**6**:2439–2457. doi:10.7150/thno.16088

[3] Albert K, Hsu HY. Carbon-based materials for photo-triggered theranostics applications. Molecules. 2016;**21**:1585. doi:10.3390/molecules21111585

[4] Chilakamarthi U, Giribabu L. Photodynamic therapy: past, present and future. The Chemical Records. 2017;**17**:1–29. doi:10.1002/tcr.201600121

[5] Dolmans DEJGJ, Fukumura D, Jain RK. Photodynamic therapy for cancer. Nature Reviews Cancer. 2003;**3**:380–387. doi:10.1038/nrc1071

[6] Castano AP, Mroz P, Hamblin MR. Photodynamic therapy and anti-tumour immunity. Nature Reviews Cancer. 2006;**6**:535–545. doi:10.1038/nrc1894

[7] Wilson BC, Patterson MS. The physics, biophysics and technology of photodynamic therapy. Physics in Medicine and Biology. 2008;**53**:R61–R109. doi:10.1088/0031-9155/53/9/R01

[8] Collins HA, Khurana M, Moriyama EH, Mariampillai A, Dahlstedt E, Balaz M, Kuimova MK, Drobizhev M, Yang VXD, Phillips D, Rebane A, Wilson BC, Anderson HL. Blood-vessel closure using photosensitizers engineered for two-photon excitation. Nature Photonics. 2008;**2**:420–424. doi:10.1038/nphoton.2008.100

[9] Calixto GM, Bernegossi J, de Freitas LM, Fontana CR, Chorilli M. Nanotechnology-based drug delivery systems for photodynamic therapy of cancer: a review. Molecules. 2016;**21**:342. doi:10.3390/molecules21030342

[10] Lang K, Mosinger J, Wagneroviá DM. Photophysical properties of porphyrinoid sensitizers non-covalently bound to host molecules; models for photodynamic therapy. Coordination Chemistry Reviews. 2004;**248**;321–350. doi:10.1016/j.ccr.2004.02.004

[11] DeRosa MC, Crutchley RJ. Photosensitized singlet oxygen and its applications. Coordination Chemistry Reviews. 2002;**233–234**:351–371. doi:10.1016/S0010-8545(02)00034-6

[12] Schweitzer C, Schmidt R. Physical mechanisms of generation and deactivation of singlet oxygen. Chemical Reviews. 2003;**103**:1685–1758. doi:10.1021/cr010371d

[13] Ogilby PR. Singlet oxygen: there is indeed something new under the sun. Chemical Society Reviews. 2010;**39**:3181–3209. doi:10.1039/B926014P

[14] Almerie MQ, Gossedge G, Wright KE, Jayne DG. Photodynamic diagnosis for detection of peritoneal carcinomatosis. Journal of Surgical Research. 2015;**195**:175–187. doi:10.1016/j.jss.2015.01.009

[15] Li B, Lin L, Lin H, Wilson BC. Photosensitized singlet oxygen generation and detection: recent advances and future perspectives in cancer photodynamic therapy. Journal of Biophotonics. 2016;**9**:1314–1325. doi:10.1002/jbio.201600055

[16] Moghissi K, Dixon K, Stringer M, Thorpe JA. Photofrin PDT for early stage oesophageal cancer: long term results in 40 patients and literature review. Photodiagnosis and Photodynamic Therapy. 2009;**6**:159–166. doi:10.1016/j.pdpdt.2009.07.026

[17] Wang S, Bromley E, Xu L, Chen JC, Keltner L. Talaporfin sodium. Expert Opinion on Pharmacotherapy. 2010;**11**:133–140. doi:10.1517/14656560903463893

[18] Tørring T, Toftegaard R, Arnbjerg J, Ogilby PR, Gothelf KV. Reversible pH-regulated control of photosensitized singlet oxygen production using a DNA i-motif. Angewandte Chemie International Edition. 2010;**49**:7923–7925. doi:10.1002/anie.201003612

[19] Op de Beeck M, Madder A. Sequence specific DNA cross-linking triggered by visible light. Journal of the American Chemical Society. 2012;**134**:10737–10740. doi:10.1021/ja301901p

[20] Tørring T, Helmig S, Ogilby PR, Gothelf KV. Singlet oxygen in DNA nanotechnology. Accounts of Chemical Research. 2014;**47**:1799–806. doi:10.1021/ar500034y

[21] Foote CS. Definition of type I and type II photosensitized oxidation. Photochemistry and Photobiology. 1991;**54**:659. doi:10.1111/j.1751-1097.1991.tb02071.x

[22] Casas A, Di Venosa G, Hasan T, Al Batlle. Mechanisms of resistance to photodynamic therapy. Current Medicinal Chemistry. 2011;**18**:2486–2515. doi:10.2174/092986711795843272

[23] Dumont E, Monari A. Understanding DNA under oxidative stress and sensitization: the role of molecular modeling. Frontiers in Chemistry. 2015;**3**:43. doi:10.3389/fchem.2015.00043

[24] Nam G, Rangasamy S, Ju H, Samson AA, Song JM. Cell death mechanistic study of photodynamic therapy against breast cancer cells utilizing liposomal delivery of 5,10,15,20-tetrakis(benzo[b]thiophene) porphyrin. Journal of Photochemistry and Photobiology B: Biology. 2017;**166**:116–125. doi:10.1016/j.jphotobiol.2016.11.006

[25] Tabrizi L, Chiniforoshan H. New Ru(II) pincer complexes: synthesis, characterization and biological evaluation for photodynamic therapy. Dalton Transactions. 2016;**45**:18333–18345. doi:10.1039/C6DT03502G

[26] Boodram S, Bullock JL, Rambaran VH, Holder AA. The use of inorganic compounds in photodynamic therapy: improvements in methods and photosensitizer design. Recent Patents on Nanotechnology. 2017;**11**:3–14. doi:10.2174/1872210510666160425121512

[27] Soriano J, Mora-Espí I, Alea-Reyes ME, Pérez-García L, Barrios L, Ibáñez E, Nogués C. Cell death mechanisms in tumoral and non-tumoral human cell lines triggered by photodynamic treatments: apoptosis, necrosis and parthanatos. Scientific Reports. 2017;**7**:41340. doi:10.1038/srep41340

[28] Burrows CJ, Muller JG. Oxidative nucleobase modifications leading to strand scission. Chemical Reviews. 1998;**98**:1109–1151. doi:10.1021/cr960421s

[29] Kawanishi S, Hiraku Y, Oikawa S. Mechanism of guanine-specific DNA damage by oxidative stress and its role in carcinogenesis and aging. Mutation Research. 2001;**488**:65–76. doi:10.1016/S1383-5742(00)00059-4

[30] Hiraku Y, Ito K, Hirakawa K, Kawanishi S. Photosensitized DNA damage and its protection via a novel mechanism. Photochemistry and Photobiology. 2007;**83**:205–212. doi:10.1562/2006-03-09-IR-840

[31] Namikawa T, Yatabe T, Inoue K, Shuin T, Hanazaki K. Clinical applications of 5-aminolevulinic acid-mediated fluorescence for gastric cancer. World Journal of Gastroenterology. 2015;**21**:8769–8775. doi:10.3748/wjg.v21.i29.8769

[32] Ishikawa T, Takahashi K, Ikeda N, Kajimoto Y, Hagiya Y, Ogura S, Miyatake S, Kuroiwa T. Transporter-mediated drug interaction strategy for 5-aminolevulinic acid (ALA)-based photodynamic diagnosis of malignant brain tumor: molecular design of ABCG2 inhibitors. Pharmaceutics. 2011;**3**:615–635. doi:10.3390/pharmaceutics3030615

[33] Harmatys KM, Musso AJ, Clear KJ, Smith BD. Small molecule additive enhances cell uptake of 5-aminolevulinic acid and conversion to protoporphyrin IX. Photochemistry and Photobiological Sciences. 2016;**15**:1408–1416. doi:10.1039/C6PP00151C

[34] Yang X, Palasuberniam P, Kraus D, Chen B. Aminolevulinic acid-based tumor detection and therapy: molecular mechanisms and strategies for enhancement. International Journal of Molecular Sciences. 2015;**16**:25865–25880. doi:10.3390/ijms161025865

[35] Ishizuka M, Abe F, Sano Y, Takahashi K, Inoue K, Nakajima M, Kohda T, Komatsu N, Ogura S, Tanaka T. Novel development of 5-aminolevurinic acid (ALA) in cancer diagnoses and therapy. International Immunopharmacology. 2011;**11**:358–365. doi:10.1016/j.intimp.2010.11.029

[36] Guyotat J, Pallud J, Armoiry X, Pavlov V, Metellus P. 5-Aminolevulinic acid-protoporphyrin IX fluorescence-guided surgery of high-grade gliomas: a systematic review. Advances and Technical Standards in Neurosurgery. 2016;**43**:61–90. doi:10.1007/978-3-319-21359-0_3

[37] Huang Z, Shi S, Qiu H, Li D, Zou J, Hu S. Fluorescence-guided resection of brain tumor: review of the significance of intraoperative quantification of protoporphyrin IX fluorescence. Neurophotonics. 2017;**4**: 011011. doi:10.1117/1.NPh.4.1.011011

[38] Mowatt G, N'Dow J, Vale L, Nabi G, Boachie C, Cook JA, Fraser C, Griffiths TR. Photodynamic diagnosis of bladder cancer compared with white light cystoscopy: systematic review and meta-analysis. International Journal of Technology Assessment in Health Care. 2011;**7**:3–10. doi:10.1017/S0266462310001364

[39] Ding H, Sumer BD, Kessinger CW, Dong Y, Huang G, Boothman DA, Gao J. Nanoscopic micelle delivery improves the photophysical properties and efficacy of photodynamic therapy of protoporphyrin IX. Journal of Controlled Release. 2011;**151**:271–277. doi:10.1016/j.jconrel.2011.01.004

[40] Khan GS, Shah A, Zia-ur-Rehman, Barker D. Chemistry of DNA minor groove binding agents. Journal of Photochemistry and Photobiology B: Biology. 2012;**115**:105–118. doi:10.1016/j.jphotobiol.2012.07.003

[41] Hamilton PL, Arya DP. Natural product DNA major groove binders. Natural Product Repots. 2012;**29**:134–143. doi:10.1039/c1np00054c

[42] Hirakawa K, Nakajima S. Effect of DNA microenvironment on photosensitized reaction of water soluble cationic porphyrins. Recent Advances in DNA & Gene Sequences. 2014;**8**:35–43. doi:10.2174/2352092208666141013231434

[43] Thulasiram B, Devi CS, Kumar YP, Aerva RR, Satyanarayana S, Nagababu P. Correlation between molecular modelling and spectroscopic techniques in investigation with DNA binding interaction of ruthenium(II) complexes. Journal of Fluorescence. 2017;**27**:587–594. doi:10.1007/s10895-016-1986-x

[44] Hirakawa K. DNA damage through photo-induced electron transfer and photosensitized generation of reactive oxygen species. In: Kimura H, Suzuki A, editors. New research on DNA damage. Nova Science Publishers Inc.; 2008, pp. 197–219. ISBN 978-1-60456-581-2

[45] Hirakawa K, Ota K, Hirayama J, Oikawa S, Kawanishi S. Nile blue can photosensitize DNA damage through electron transfer. Chemical Research in Toxicology. 2015;**27**:649–655. doi:10.1021/tx400475c

[46] Hirakawa K, Kawanishi S, Hirano T. The mechanism of guanine specific photooxidation in the presence of berberine and palmatine: activation of photosensitized singlet oxygen generation through DNA-binding interaction. Chemical Research in Toxicology. 2005;**18**:1545–1552. doi:10.1021/tx0501740

[47] Hirakawa K, Hirano T. The microenvironment of DNA switches the activity of singlet oxygen generation photosensitized by berberine and palmatine. Photochemistry and Photobiology. 2008;**84**:202–208. doi:10.1111/j.1751-1097.2007.00220.x

[48] Hirakawa K, Hirano T, Nishimura Y, Arai T, Nosaka Y. Dynamics of singlet oxygen generation by DNA-binding photosensitizers. The Journal of the Physical Chemistry B. 2012;**116**:3037–3044. doi:10.1021/jp300142e

[49] Mazzini S, Bellucci MC, Mondelli R. Mode of binding of the cytotoxic alkaloid berberine with the double helix oligonucleotide d(AAGAATTCTT)$_2$. Bioorganic and Medicinal Chemisry. 2003;**11**:505–514. doi:10.1016/S0968-0896(02)00466-2

[50] Usui Y, Kamogawa K. A standard system to determine the quantum yield of singlet oxygen formation in aqueous solution. Photochemistry and Photobiology. 1974;**19**:245–247. doi:10.1111/j.1751-1097.1974.tb06506.x

[51] Barawkar DA, Ganesh KN. Fluorescent d(CGCGAATTCGCG): characterization of major groove polarity and study of minor groove interactions through a major groove semantophore conjugate. Nucleic Acids Research. 1995;**23**:159–164. PMCID: PMC306644

[52] Jin R, Breslauer KJ. Characterization of the minor groove environment in a drug-DNA complex: bisbenzimide bound to the poly[d(AT)].poly[d(AT)]duplex. Proceedings of the National Academy of Sciences of the United States of America. 1988;**85**:8939–8942. PMCID: PMC282622

[53] Tada-Oikawa S, Oikawa S, Hirayama J, Hirakawa K, Kawanishi S. DNA damage and apoptosis induced by photosensitization of 5,10,15,20-tetrakis (N-methyl-4-pyridyl)-21H,23H-porphyrin via singlet oxygen generation. Photochemistry and Photobiology. 2009;**85**:1391–1399. doi:10.1111/j.1751-1097.2009.00600.x

[54] Hirakawa K, Harada M, Okazaki S, Nosaka Y. Controlled generation of singlet oxygen by a water-soluble meso-pyrenylporphyrin photosensitizer through interaction with DNA. Chemical Communications. 2012;**48**:4770–4772. doi:10.1039/c2cc30880k

[55] Hirakawa K, Nishimura Y, Arai T, Okazaki S. Singlet oxygen generating activity of an electron donor-connecting porphyrin photosensitizer can be controlled by DNA. The Journal of the Physical Chemistry B. 2013;**117**:13490–13496. doi:10.1021/jp4072444

[56] Hirakawa K, Ito Y, Yamada T, Okazaki S. Relaxation process of the photoexcited state and singlet oxygen generating activity of water-soluble meso-phenanthrylporphyrin in a DNA microenvironment. Rapid Communication in Photoscience. 2014;**3**:81–84. doi:10.5857/RCP.2014.3.4.81

[57] Hirakawa K, Taguchi M, Okazaki S. Relaxation process of photoexcited meso-naphthylporphyrins while interacting with DNA and singlet oxygen generation. The Journal of Physical Chemistry B. 2015;**119**:13071–13078. doi:10.1021/acs.jpcb.5b08025

[58] Marcus RA. On the theory of oxidation-reduction reactions involving electron transfer. I. The Journal of Chemical Physics. 1956;**24**:966–978. doi:10.1063/1.1742723

[59] Marcus RA, Sutin N. Electron transfers in chemistry and biology. Biochimica et Biophysica Acta. 1985;**811**:265–322. doi:10.1016/0304-4173(85)90014-X

[60] Wasielewski MR. Photoinduced electron transfer in supramolecular systems for artificial photosynthesis. Chemical Reviews. 1992;**92**:435–461. doi:10.1021/cr00011a005

[61] Kobori Y, Yamauchi S, Akiyama K, Tero-Kubota S, Imahori H, Fukuzumi S, Norris Jr. JR. Primary charge-recombination in an artificial photosynthetic reaction. Proceedings of the National Academy of Sciences of the United States of America. 2005;**102**:10017–10022. doi:10.1073/pnas.0504598102

[62] Kubo M, Mori Y, Otani M, Murakami M, Ishibashi M, Yasuda M, Hosomizu K, Miyasaka H, Imahori H, Nakashima S. Ultrafast photoinduced electron transfer in directly linked porphyrin-ferrocene dyads. The Journal of Physical Chemistry A. 2007;**111**:5136–5143. doi:10.1021/jp071546b